Skin permeation studies of chromium species – Evaluation of a reconstructed human epidermis model

Toxicology in Vitro 91 (2023) 105636

Contents lists available at ScienceDirect

Toxicology in Vitro

journal homepage: www.elsevier.com/locate/toxinvit

Skin permeation studies of chromium species – Evaluation of a reconstructed human epidermis model

L. Hagvall [a,b,*], M. Munem [c], M. Hoang Philipsen [c], M. Dowlatshahi Pour [a], Y. Hedberg [d,e,f], P. Malmberg [c]

[a] Department of Dermatology and Venereology, Institute of Clinical Sciences, Sahlgrenska Academy, University of Gothenburg, Gothenburg, Sweden
[b] Department of Occupational and Environmental Medicine, Lund University, Lund, Sweden
[c] Department of Chemistry and Chemical Engineering, Chalmers University of Technology, Gothenburg, Sweden
[d] Department of Chemistry, The University of Western Ontario, 1151 Richmond St., London, Ontario N6A 5B7, Canada
[e] Surface Science Western, The University of Western Ontario, 999 Collip Circle, London, Ontario N6G 0J3, Canada
[f] Lawson Health Research Institute, London, Ontario N6C 2R5, Canada

ARTICLE INFO

Editor: Dr. P Jennings

ABSTRACT

A reconstructed human epidermis (RHE) model, the EpiDerm, was investigated and compared to human skin *ex vivo* regarding tissue penetration and distribution of two chromium species, relevant in both occupational and general exposure in the population. Imaging mass spectrometry was used in analysis of the sectioned tissue. The RHE model gave similar results compared to human skin *ex vivo* for skin penetration of Cr^{VI}. However, the penetration of Cr^{III} into the tissue of the RHE model compared to human skin *ex vivo* differed markedly, such that in the RHE model the Cr^{III} species accumulated in the tissue layer corresponding to *stratum corneum* whereas in human skin *ex vivo*, the Cr^{III} species penetrated evenly through the skin tissue. Further, skin lipids such as cholesterol were less abundant in the RHE model compared to the human skin tissue. Results presented here indicate that the RHE models do not possess the same fundamental properties as human skin tissue. As the RHE models appear to be able to give false negative results, experiments using RHE models for the study of skin penetration should be evaluated with caution.

1. Introduction

Chromium is an element with complex chemistry and toxicity. While having several oxidation states, the most discussed in terms of toxicology are trivalent (Cr^{III}) and hexavalent (Cr^{VI}) chromium. Exposure to Cr^{VI} is an important risk factor for the development of lung cancer in occupational settings, *i.e.* in welding (Kauppinen et al., 2000; Stridsklev et al., 1993). Cr^{VI} can also cause allergic contact dermatitis. Occupational skin exposure to chromium species occurs mainly through wet cement, leather gloves and chromium plating (Bregnbak et al., 2015). Within the EU, Cr^{VI} in cement and leather is regulated by the REACH directive (301/2014). However, the content of Cr^{III} in leather is not regulated. Under typical environmental conditions, Cr^{VI} can form from Cr^{III}, present in leather, in significant amounts (Hedberg and Liden, 2016). In addition, exposure to Cr^{VI} occurs still from cement that fully complies with current European regulations (Hedberg et al., 2014). Skin exposure to both Cr^{III} and Cr^{VI} is thus still frequent.

Chromium is a common cause of irritant and allergic contact dermatitis both in occupational and domestic settings (Bregnbak et al., 2015). In order to induce contact allergy, which is a T-cell mediated immune response, sensitizers are believed to first penetrate the skin barrier through the stratum corneum, reaching into the epidermis where they bind to skin proteins or other macromolecules thus forming antigens distinguishable to dendritic cells (Karlberg et al., 2008). Previous animal studies of the sensitization potency of chromium species have suggested Cr^{III} to be the actual hapten in chromium contact allergy, although the skin penetration of Cr^{III} in guinea pigs was found to be very low (Siegenthaler et al., 1983). Patch test and use test studies in patients with contact allergy to Cr^{VI} have shown that Cr^{III} is a relevant hapten in chromium contact allergy (Hansen et al., 2003; Hedberg et al., 2018). Further, Cr^{VI} has been shown to induce an innate immune response, which is necessary for the development of both irritant and allergic contact dermatitis (Adam et al., 2017).

* Corresponding author at: Department of Dermatology and Venereology, Institute of Clinical Sciences, Sahlgrenska Academy, University of Gothenburg, Gothenburg, Sweden.
E-mail address: lina.hagvall@med.lu.se (L. Hagvall).

https://doi.org/10.1016/j.tiv.2023.105636
Received 9 March 2023; Received in revised form 5 June 2023; Accepted 24 June 2023
Available online 26 June 2023

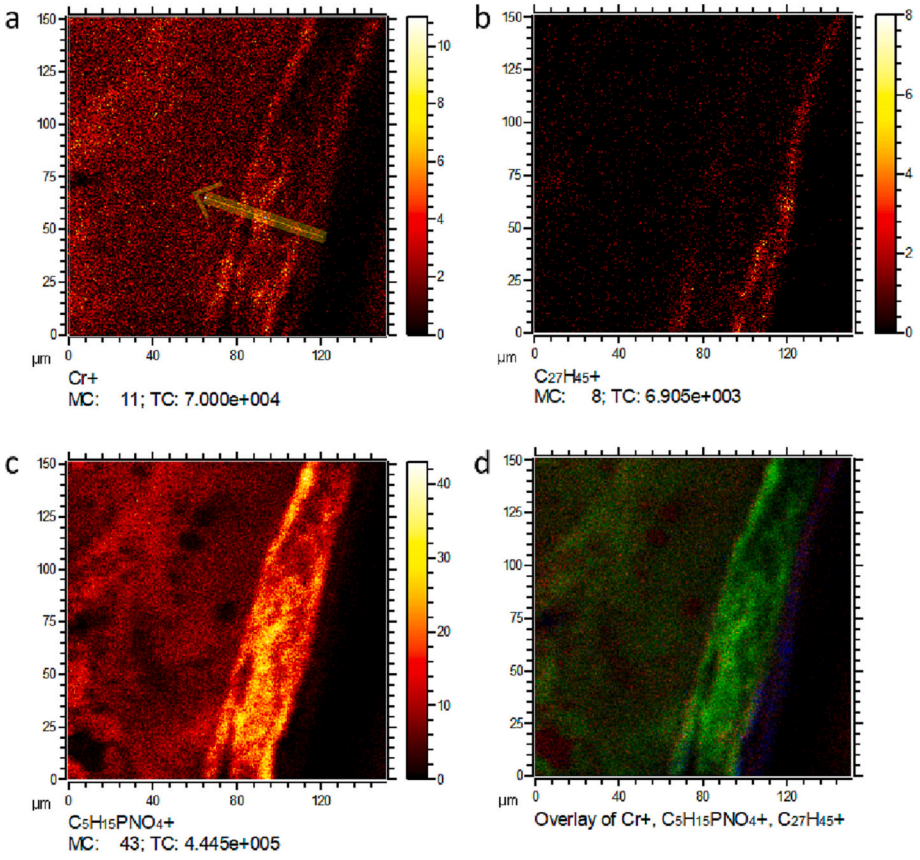

Fig. 1. ToF-SIMS ion images from a section of RHE exposed to Cr^{VI}, showing the distribution pattern of a) chromium ion b) cholesterol c) phosphatidylcholine headgroup and d) RGB colour overlay ion images of chromium ions in red, phosphatidylcholine headgroup in green and cholesterol in blue. Field of view of 150 × 150 µm. The yellow arrow in a) shows the direction of penetration.

Previously, skin penetration of metal salts has been studied using human skin *ex vivo* mounted in diffusion cells. The detail of the analysis has been limited to the receptor fluid and the different skin layers in their entirety as the skin tissue has been divided using thermal methods and homogenized. Gammelgaard et al. found higher skin permeation of Cr^{VI} than of Cr^{III} (Gammelgaard et al., 1992). In exposure to cement suspensions with and without iron sulphate, chromium species were detected in dermis to a larger extent than the epidermis using atomic absorption spectrometry (Fullerton et al., 1993). No chromium species could be detected in the receptor fluid. Van Lierde et al. detected Cr^{VI} but not Cr^{III} in the receptor fluid of human skin mounted in diffusion cells using inductively coupled plasma-sector field mass spectrometry (Van Lierde et al., 2006). Higher amounts of Cr^{VI} than Cr^{III} were detected in the skin tissue, however, no detailed analysis was performed of different skin layers.

More recently, reconstructed human epidermis models (RHE) have been used in order to investigate skin permeation of drugs, such as cortisones and antimycotics, showing that the flux through the skin of these organic compounds was higher than for *ex vivo* human skin tissue (Schmook et al., 2001). RHEs have also been used in contact allergy research, investigating changes in gene expression and interleukin production (Gibbs et al., 2018; Rodrigues Neves and Gibbs, 2021). The sensitization potency of metal salts has been investigated using interleukin-18 production in RHE exposed to a series of sensitizers, both organic compounds and metal salts. The sensitization potency of several metal salts could not be determined and the degree of penetration of these compounds into the tissue was questioned (Gibbs et al., 2018). The issue of skin penetration was however not further investigated.

Mass spectrometry imaging (time of flight secondary ion mass spectrometry - ToF-SIMS) presents an alternative method for the study of skin distribution and penetration of metal ion sensitizers. This technique allows direct visualization of the distribution of the metal ions in skin tissue, simultaneously with endogenous compounds of the skin. We recently presented a mass spectrometry imaging-based alternative to these methods, providing detailed qualitative data on distribution of metal ions in the skin tissue and colocalization with endogenous compounds (Hagvall et al., 2021; Malmberg et al., 2018; Munem et al., 2021). Recent method development allows the analysis to be performed at nanometer-resolution, while maintaining a sufficient mass resolution (Henss et al., 2018).

The aim of this study was to investigate distribution and penetration of Cr^{VI} and Cr^{III} species in a reconstructed human epidermis model compared to human skin *ex vivo*, focusing on skin uptake and distribution in the skin tissue layers. The previously used methodology of analysis of the receptor fluid of the diffusion cell was combined with imaging mass spectrometry, providing a detailed analysis of chromium species distribution in skin tissue.

2. Materials and methods

Chemicals. Ammonium formate (Sigma Aldrich, St Louis, MO, USA) was dissolved in deionized water to a concentration of 0.15 M to serve as the buffer solution. Potassium dichromate (Cr^{VI}) and chromium (Cr^{III}) chloride hexahydrate (Sigma Aldrich, St Louis, MO, USA) were dissolved in ammonium formate buffer solutions to a concentration of 0.03 M, respectively.

Human skin tissue collection. Leftover full-thickness human skin was collected from breast reduction surgery at the Department of Plastic Surgery, Sahlgrenska University Hospital, and prepared as previously described (Hagvall et al., 2021). Donors gave consent to the use of their

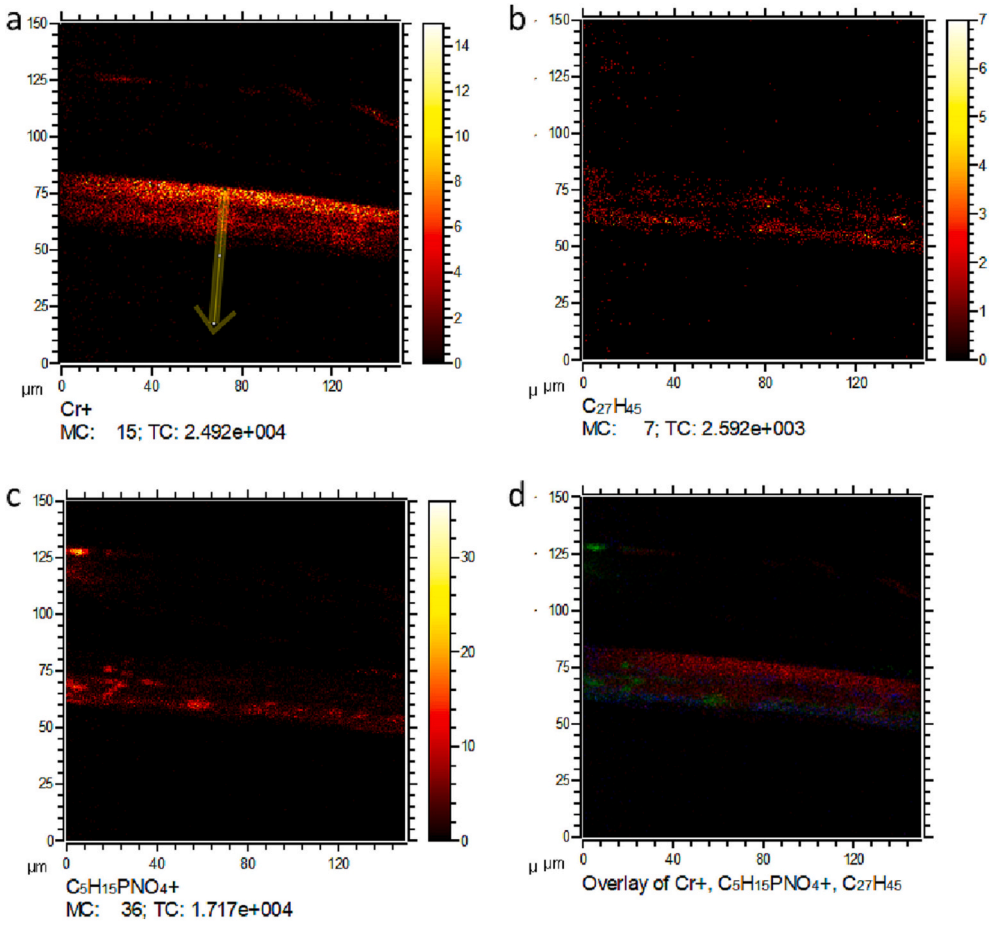

Fig. 2. ToF-SIMS ion images from a section of RHE exposed to Cr^{III}, showing the distribution pattern of a) chromium ion b) cholesterol c) phosphatidylcholine headgroup and d) RGB colour overlay ion images of chromium ions in red, phosphatidylcholine headgroup in green and cholesterol in blue. Field of view of 150 × 150 µm. The yellow arrow in a) shows the direction of penetration.

surgical waste. Tissue was made anonymous upon collection in agreement with routines approved by the Regional Ethical Review Board in Gothenburg.

Reconstructed human epidermis. The EpiDerm™ skin model was purchased from MatTek Life Sciences Inc. and used within 24 h of delivery, in compliance with instructions from the company.

Exposure experiment. Sample treatment and diffusion cell experiments were performed according to our previous work (Hagvall et al., 2021). Accordingly, diffusion cells (Franz type, Laboratory Glass Apparatus, Berkley, CA, exposed surface area 1 cm^2) were arranged such that skin samples ($n = 2$) and skin model samples (n = 2) were exposed to 1 ml of potassium dichromate (Cr^{VI}) solution (0.03 M) and chromium (Cr^{III}) chloride hexahydrate (0.03 M) in sodium formate buffer (0.15 M), respectively. One sample each of human skin *ex vivo* and the EpiDerm skin model were exposed to ammonium formate buffer solution and served as controls *i.e.*, there were 2 exposed samples and 1 control for each experiment. The exposure time was 24 h, and the temperature was kept at 4 °C. At removal, tissue samples were gently rinsed with distilled water. Diffusion cells, utensils and sample vials for receptor and donor solutions were all acid washed (10% HNO_3, 24 h) as previously described (Hedberg and Liden, 2016) in order to avoid contamination of the samples. Plastic utensils for handling the skin tissue were used as much as possible to avoid chromium contamination. Exposure of human skin to Cr^{III} was performed in a previous study (Hagvall et al., 2021). Line scan analysis was performed again, showing the same pattern of tissue distribution of Cr^{III}.

Tissue preparation for ToF-SIMS. Skin tissue samples were frozen in isopentane after removal from the diffusion cells. The frozen skin tissue sections were then sectioned vertically at a thickness of 10 µm. Four slices from the middle of the sample were collected and mounted on glass slides for ToF-SIMS analysis. One duplicate glass slide was prepared in each skin sectioning operation. Sections were freeze dried prior to ToF-SIMS analysis.

ToF-SIMS analysis. The ToF-SIMS surface analysis was carried out using the ToF. SIMS 5 instrument (ION-ToF GmbH, Münster, Germany) equipped with a Bi cluster ion gun as a primary ion source. Mass spectra in positive ion mode were acquired by using the 25 keV Bi_3^+ primary ion source. To acquire images with high spatial respective mass resolution, the delayed extraction mode was used (Vanbellingen et al., 2015). The pulsed primary ion currents were in the range of 0.14pA ~ 0.17pA. Areas of about 150 × 150 µm on the skin section were selected with a raster of 256 × 256-pixels and analyzed with 1000 raster scans. Four different sections from the specimens of control and treated samples were analyzed, respectively. The spectra were internally calibrated to signals of common fragments as $[C]^+$, $[CH_2]^+$, $[CH_3]^+$, $[C_5H_{15}PNO_4]^+$, $[C_{27}H_{45}]^+$. The software SURFACELAB (version 7.1, ION-TOF) was used to process, record, analyze and evaluate images and mass spectra.

Analysis of Cr^{VI} in donor and receptor fluids. Cr^{VI} was analyzed using spectrophotometry (Jenway 6300, Staffordshire, UK), during which a reaction producing a pink colour (maximum peak at 540 nm) was utilized to quantify Cr^{VI} in aqueous samples. More details about the analysis are given in previous work (Hedberg et al., 2019). Five replicate readings for duplicate samples of donor and receptor fluids (after the exposure experiment) and corresponding blank fluids (no added Cr^{VI}) were performed. The five-point calibration curve was linear and up to 1 mg/l. The blank concentrations were negligible, and they were

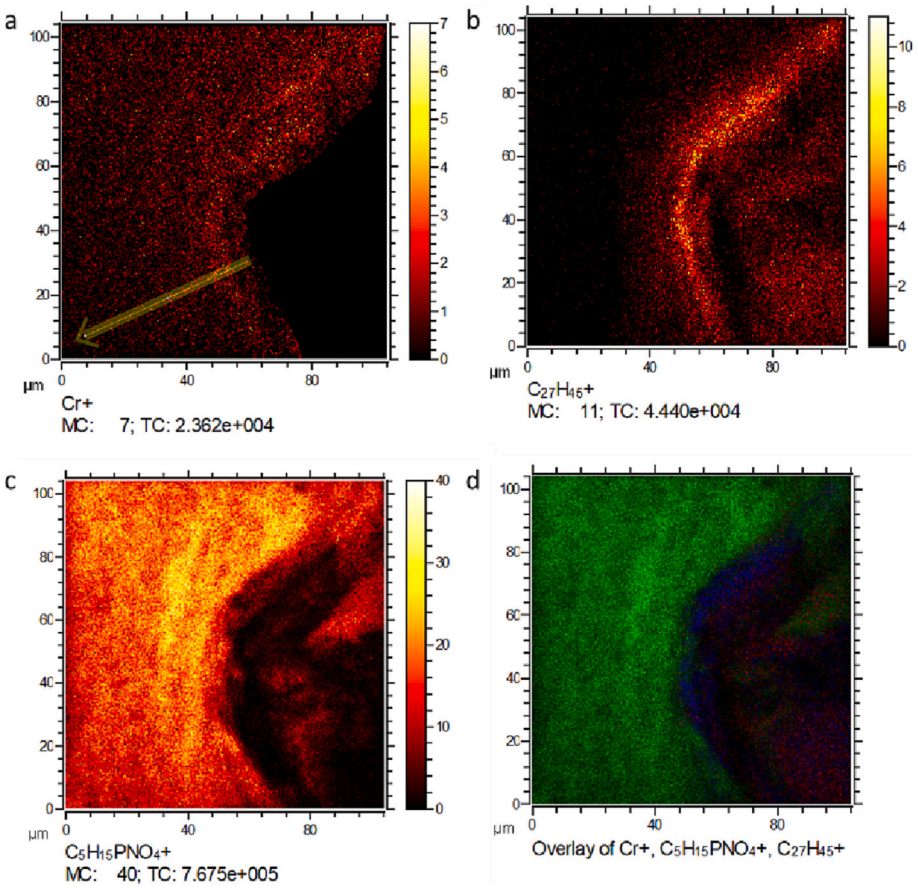

Fig. 3. ToF-SIMS ion images from a section of human skin *ex vivo* exposed to Cr^{VI}, showing the distribution pattern of a) chromium ion b) cholesterol c) phosphatidylcholine headgroup and d) RGB colour overlay ion images of chromium ions in red, phosphatidylcholine headgroup in green and cholesterol in blue. Field of view of 100 × 100 µm. The yellow arrow in a) shows the direction of penetration.

subtracted if positive. The samples were diluted with a blank sample to fit within the calibration curve, and all samples significantly exceeded the detection limit (60 µg/l).

3. Results and discussion

In this study we chose the EpiDerm™ Reconstructed Human Epidermis (RHE) model as a representative model for the evaluation of the penetration of chromium species in RHE models compared to human skin tissue *ex vivo*, as it is composed of normal human keratinocytes and is one of the more widely used models among the 6 RHE models approved by the OECD for testing of skin irritation (OECD, 2021). The EpiDerm™ RHE consists of a "dermis" with fibroblasts embedded in a collagen I matrix, an "epidermis", which is comprised of stratified, differentiated keratinocytes and a functional basement membrane, which separates epidermis from dermis (OECD, 2021).

The distributions of Cr^{VI} and Cr^{III} in RHE exposed to each ion individually are presented in Figs. 1 and 2, respectively. The figures show single-ion images of chromium, cholesterol, and the phosphatidylcholine headgroup. Cholesterol is one of the most abundant lipids of the skin, including stratum corneum, and is used here as a general marker for skin tissue. The phosphatidylcholine headgroup is a fragment of all major PCs in cell membranes and can be used as a marker to separate the *stratum corneum* from the epidermis. Both Cr^{VI} and Cr^{III} penetrated into the RHE layer corresponding to the *stratum corneum*, however, Cr^{VI} penetrated further and was evenly distributed in the tissue (Fig. 1). The Cr^{III} signal diminished rapidly in the border between the RHE layer corresponding to the *stratum corneum* and epidermis. No signal from any chromium species was detected in the controls (Figs. S1 and S2).

The distribution of Cr^{VI} in human skin *ex vivo* is presented in Fig. 3. Cr^{VI} was evenly distributed in the tissue. The signals were generally lower compared to Cr^{VI} exposure in the RHE model. The pattern of tissue penetration of Cr^{VI} in the RHE model was thus consistent with the results from human skin *ex vivo*. This chromium species was evenly distributed through the skin layers within the tissue area analyzed. No signal of Cr^{VI} was detected in the control (Fig. S3).

Analysis of Cr^{VI} concentrations in the donor fluids indicated no significant (>50%) reduction to Cr^{III} despite storage and transport times between exposure experiment and chemical analysis, they were lower (about half) in the fluids in contact with the human skin *ex vivo* than the RHE model. This might indicate a reduction of Cr^{VI} due to the presence of certain biomolecules in skin, which are lacking or present in low abundance in the RHE model (Nikpour and Hedberg, 2021; Wright et al., 2022). Most importantly, the percentage that penetrated the human skin *ex vivo* and RHE model was <0.1% and between 1 and 10%, respectively. This further supports that human skin *ex vivo* has a reduction capacity for Cr^{VI}, resulting in lower penetration rates.

When exposed to Cr^{VI}, the receptor fluids of the RHE model appeared yellow and orange, which most likely correspond to CrO_4^{2-} and $Cr_2O_7^{2-}$, respectively (Kozlica and Milosev, 2021). In contrast, the receptor fluid of the human skin *ex vivo* appeared pink, which indicates the formation of trivalent Cr^{III} species, either pink Cr^{III}-chloride complexes (Elving and Zemel, 1957) or purple, violet, or red Cr^{III}-amino acid complexes (Budiasih et al., 2013; Mizuochi et al., 1971). This observation also supports a higher reduction capacity of Cr^{VI} for the human skin tissue compared with the RHE model.

In order to evaluate the difference in skin penetration of Cr^{VI} and Cr^{III} in the RHE model compared to human skin *ex vivo*, line scan analysis was

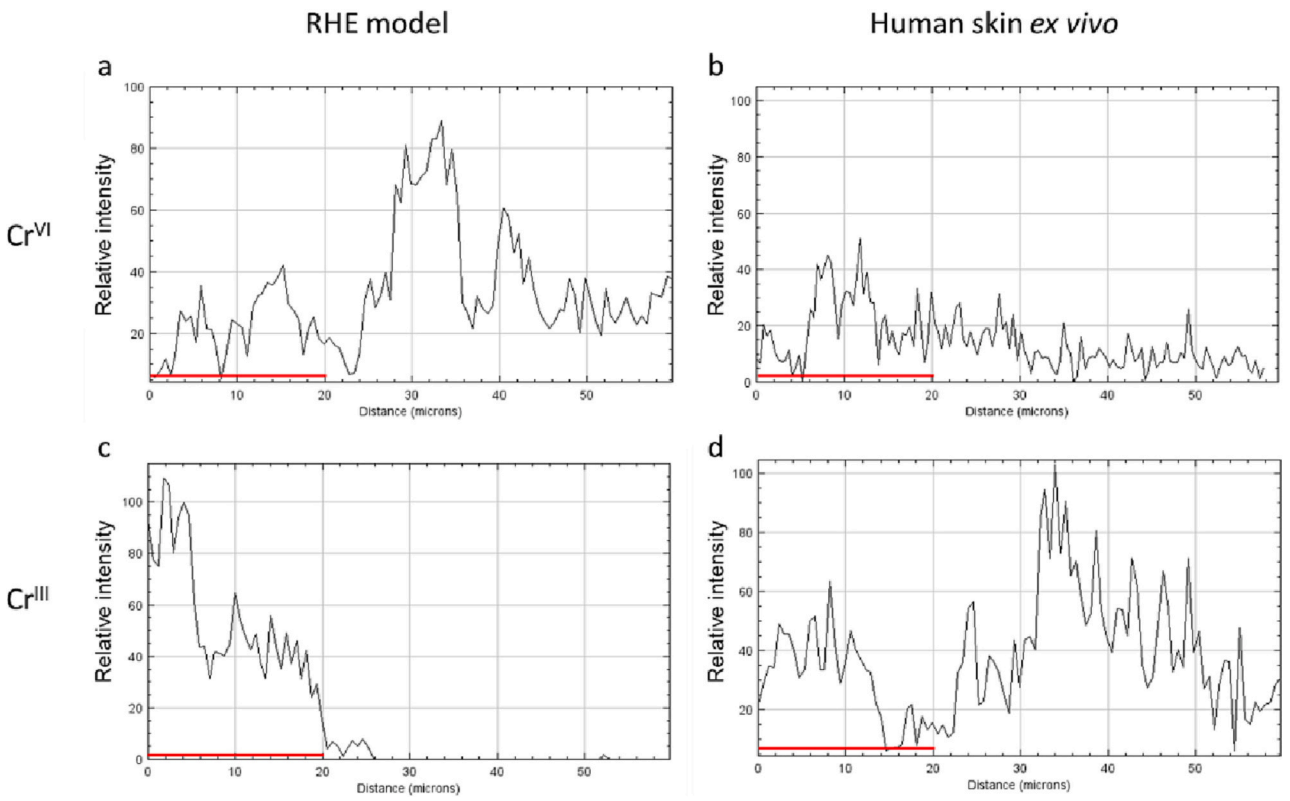

Fig. 4. Line scan analysis of ToF-SIMS ion images of tissue sections of a) RHE model exposed to Cr^{VI}, b) human skin *ex vivo* exposed to Cr^{VI}, c) RHE model exposed to Cr^{III} and d) human skin *ex vivo* exposed to Cr^{III}, showing the ion intensity of chromium species *versus* distance from the tissue surface. Stratum corneum layer thickness (20 μm) is marked with a red line along the x-axes. The data for each graph is based on the mean of line scans performed over 10 pixels (yellow lines in Figs. 1–3 a). Imaging data constituting the basis for the analysis in d) are previously published, Fig. 1e in (Hagvall et al., 2021).

performed. Here, a mean of the signal for chromium over a width of 10 pixels was plotted against the tissue depth for RHE and human skin *ex vivo* exposed to Cr^{III} and Cr^{VI}, respectively. Results are shown in Fig. 4. Results of exposure of human skin *ex vivo* to Cr^{III} has been previously published, Fig. 1e and 2b in (Hagvall et al., 2021). While the pattern of skin penetration of Cr^{VI} is similar between the RHE model and the human skin *ex vivo*, the pattern of skin penetration of Cr^{III} is not. Here, the RHE model indicates that Cr^{III} will not penetrate further than the layer corresponding to the *stratum corneum*, however, the results from the human skin *ex vivo* indicate that Cr^{III} is able to penetrate well into the epidermis.

In comparing the results of skin uptake and penetration of Cr^{III} and of Cr^{VI} in human skin *ex vivo*, the results are consistent with previous studies of skin penetration, as far as Cr^{VI} is generally seen to penetrate through the skin to a larger extent. However, Gammelgaard et al. observed a larger accumulation of Cr^{VI} in various skin layers compared to Cr^{III}, and observed an about 10-fold difference in favour of Cr^{VI} (Gammelgaard et al., 1992). This was also observed by Van Lierde et al., detecting about 10 times more Cr^{VI} in the skin layers compared to Cr^{III}, analyzed after separation and homogenization of the skin layers (Van Lierde et al., 2006). Further Van Lierde did not detect Cr^{III} in the receptor fluid at all. In both these studies, a longer exposure time was used, and analysis methods were less sensitive than in the present study. The present study shows that although Cr^{III} does not penetrate through the skin to the same extent as Cr^{VI}, it penetrates into human skin and is bioavailable in the upper skin layers.

In previous studies of penetration of topical drugs in RHE models compared to human cadaver skin and pig skin, all investigated drugs showed higher penetration through the RHE model (Schmook et al., 2001). Schmook et al. concluded that the barrier properties of the RHE models used are weak. Results from the present study only partly correlate with these previous findings. However, here, metal species were investigated instead of organic compounds such as topical drugs.

In more recent studies on the sensitizing capacity of metals using RHE models, Cr^{III} failed to induce a response (Gibbs et al., 2018). Gibbs et al. suggested that Cr^{III} is unable to penetrate the layer corresponding to *stratum corneum* in the RHE model. Results from the present study support this theory. However, in comparison with results from exposure of human skin *ex vivo*, the pattern of skin penetration of Cr^{III} is very different from the RHE model. Although there is differentiation of the keratinocytes, towards the tissue surface, a layer directly corresponding to the *stratum corneum* is not formed in the RHE model. Further, skin lipids such as cholesterol are less abundant in the RHE model compared to the human skin tissue (Figs. 1–3). Differences in lipid profiles between human skin and skin models have been observed previously (Netzlaff et al., 2007). This is in particular important for the penetration properties of Cr^{III} species, which increase when bound to organic ligands due to a change in charge and higher solubility (Nikpour and Hedberg, 2021).

Results presented here indicate that the RHE models do not possess the same fundamental properties as human skin tissue. If these differences always resulted in a worst-case scenario when using RHE models, it would not be a significant risk for hazard and risk assessments of chemical substances. However, as the RHE models appeared to give false negative results in the case of Cr^{III} in this study, experiments using RHE models should be evaluated with caution.

Funding

The Swedish skin foundation (Grant No.: 3037/2020:1 and 2906/2019:1), Canada Research Chairs Program (Grant No.: 950–233099), Wolfe-Western fellowship, Canada (Grant No.: 2020) and Swedish Fund

for Research Without Animal Experiments (Grant No.: F2021–0004).

Declaration of Competing Interest

The authors hereby declare that there are no conflicts of interest.

Data availability

Data will be made available on request.

Acknowledgement

Zheng Wei (KTH Royal Institute of Technology and the University of Western Ontario) is highly acknowledged for assistance in chemical analysis. Ann-Charlott Lindberg is gratefully acknowledged for sectioning of tissue samples.

Appendix A. Supplementary data

Supplementary data to this article can be found online at https://doi.org/10.1016/j.tiv.2023.105636.

References

301/2014, C.R.E.N, 2014. Amending annex XVII to regulation (EC) no 1907/2006 of the European Parliament and of the council on the registration, evaluation, authorisation and restriction of chemicals (REACH) as regards chromium VI compounds. Off. J. Eur. Union 57, 1–20.

Adam, C., Wohlfarth, J., Haussmann, M., Sennefelder, H., Rodin, A., Maler, M., Martin, S. F., Goebeler, M., Schmidt, M., 2017. Allergy-inducing chromium compounds trigger potent innate immune stimulation via ROS-dependent Inflammasome activation. J. Investig. Dermatol. 137, 367–376.

Bregnbak, D., Johansen, J.D., Jellesen, M.S., Zachariae, C., Menne, T., Thyssen, J.P., 2015. Chromium allergy and dermatitis: prevalence and main findings. Contact Dermatitis 73, 261–280.

Budiasih, K.S., Anwar, C., Santosa, S.J., Ismail, H., 2013. Synthesis and Characterization of Chromium (III) Complexes with L-Glutamic Acid, glycine and L-Cysteine, Proceedings of World Academy of Science, Engineering and Technology. World Academy of Science, Engineering and Technology (WASET), p. 1909.

Elving, P.J., Zemel, B., 1957. Absorption in the ultraviolet and visible regions of chloroaquochromium (III) ions in acid media. J. Am. Chem. Soc. 79, 1281–1285.

Fullerton, A., Gammelgaard, B., Avnstorp, C., Menne, T., 1993. Chromium content in human skin after in vitro application of ordinary cement and ferrous-sulphate-reduced cement. Contact Dermatitis 29, 133–137.

Gammelgaard, B., Fullerton, A., Avnstorp, C., Menne, T., 1992. Permeation of chromium salts through human skin in vitro. Contact Dermatitis 27, 302–310.

Gibbs, S., Kosten, I., Veldhuizen, R., Spiekstra, S., Corsini, E., Roggen, E., Rustemeyer, T., Feilzer, A.J., Kleverlaan, C.J., 2018. Assessment of metal sensitizer potency with the reconstructed human epidermis IL-18 assay. Toxicology 393, 62–72.

Hagvall, L., Pour, M.D., Feng, J., Karma, M., Hedberg, Y., Malmberg, P., 2021. Skin permeation of nickel, cobalt and chromium salts in ex vivo human skin, visualized using mass spectrometry imaging. Toxicol. in Vitro 76, 105232.

Hansen, M.B., Johansen, J.D., Menne, T., 2003. Chromium allergy: significance of both Cr(III) and Cr(VI). Contact Dermatitis 49, 206–212.

Hedberg, Y.S., Liden, C., 2016. Chromium(III) and chromium(VI) release from leather during 8 months of simulated use. Contact Dermatitis 75, 82–88.

Hedberg, Y.S., Gumulka, M., Lind, M.L., Matura, M., Liden, C., 2014. Severe occupational chromium allergy despite cement legislation. Contact Dermatitis 70, 321–323.

Hedberg, Y.S., Erfani, B., Matura, M., Liden, C., 2018. Chromium(III) release from chromium-tanned leather elicits allergic contact dermatitis: a use test study. Contact Dermatitis 78, 307–314.

Hedberg, Y.S., Wei, Z., Moncada, F., 2019. Chromium(III), chromium(VI), and cobalt release from leathers produced in Nicaragua. Contact Dermatitis 80, 149–155.

Henss, A., Otto, S.K., Schaepe, K., Pauksch, L., Lips, K.S., Rohnke, M., 2018. High resolution imaging and 3D analysis of ag nanoparticles in cells with ToF-SIMS and delayed extraction. Biointerphases 13, 03B410.

Karlberg, A.T., Bergstrom, M.A., Borje, A., Luthman, K., Nilsson, J.L.G., 2008. Allergic contact dermatitis-formation, structural requirements, and reactivity of skin sensitizers. Chem. Res. Toxicol. 21, 53–69.

Kauppinen, T., Toikkanen, J., Pedersen, D., Young, R., Ahrens, W., Boffetta, P., Hansen, J., Kromhout, H., Maqueda Blasco, J., Mirabelli, D., de la Orden-Rivera, V., Pannett, B., Plato, N., Savela, A., Vincent, R., Kogevinas, M., 2000. Occupational exposure to carcinogens in the European Union. Occup. Environ. Med. 57, 10–18.

Kozlica, D., Milosev, I., 2021. Does Cr 6+ really exist? Difference between charge and oxidation state and how to record them. Corrosion 77, 696–699.

Malmberg, P., Guttenberg, T., Ericson, M.B., Hagvall, L., 2018. Imaging mass spectrometry for novel insights into contact allergy - a proof-of-concept study on nickel. Contact Dermatitis 78, 109–116.

Mizuochi, H., Uehara, A., Kyuno, E., Tsughiya, R., 1971. The chromium (III) complexes with natural α-amino acids. Bull. Chem. Soc. Jpn. 44, 1555–1560.

Munem, M., Djuphammar, A., Sjolander, L., Hagvall, L., Malmberg, P., 2021. Animal-free skin permeation analysis using mass spectrometry imaging. Toxicol. in Vitro 71, 105062.

Netzlaff, F., Kaca, M., Bock, U., Haltner-Ukomadu, E., Meiers, P., Lehr, C.M., Schaefer, U. F., 2007. Permeability of the reconstructed human epidermis model Episkin in comparison to various human skin preparations. Eur. J. Pharm. Biopharm. 66, 127–134.

Nikpour, S., Hedberg, Y.S., 2021. Using chemical speciation modelling to discuss variations in patch test reactions to different aluminium and chromium salts. Contact Dermatitis 85, 415–420.

OECD, 2021. OECD Guideline for the Testing of Chemicals, Section 4, Guideline no 439. In Vitro Skin Irritation: Reconstructed Human Epidermis Test Method. OECD Publishing, Paris.

Rodrigues Neves, C., Gibbs, S., 2021. Progress on reconstructed human skin models for allergy research and identifying contact sensitizers. Curr. Top. Microbiol. Immunol. 430, 103–129.

Schmook, F.P., Meingassner, J.G., Billich, A., 2001. Comparison of human skin or epidermis models with human and animal skin in in-vitro percutaneous absorption. Int. J. Pharm. 215, 51–56.

Siegenthaler, U., Laine, A., Polak, L., 1983. Studies on contact sensitivity to chromium in the guinea pig. The role of valence in the formation of the antigenic determinant. J. Investig. Dermatol. 80, 44–47.

Stridsklev, I.C., Hemmingsen, B., Karlsen, J.T., Schaller, K.H., Raithel, H.J., Langard, S., 1993. Biologic monitoring of chromium and nickel among stainless steel welders using the manual mental arc method. Int. Arch. Occup. Environ. Health 65, 209–219.

Van Lierde, V., Chery, C.C., Roche, N., Monstrey, S., Moens, L., Vanhaecke, F., 2006. In vitro permeation of chromium species through porcine and human skin as determined by capillary electrophoresis-inductively coupled plasma-sector field mass spectrometry. Anal. Bioanal. Chem. 384, 378–384.

Vanbellingen, Q.P., Elie, N., Eller, M.J., Della-Negra, S., Touboul, D., Brunelle, A., 2015. Time-of-flight secondary ion mass spectrometry imaging of biological samples with delayed extraction for high mass and high spatial resolutions. Rapid Commun. Mass Spectrom. 29, 1187–1195.

Wright, A., Laundry-Mottiar, L., Hedberg, Y.S., 2022. The ability of sweat and buffer solutions to reduce hexavalent chromium of relevance for leather extraction. Regul. Toxicol. Pharmacol. 133, 105222.